JOURNAL OF GENERAL VIROLOGY

RESEARCH ARTICLE

Khan *et al.*, *Journal of General Virology* 2023;104:001888
DOI 10.1099/jgv.0.001888

MICROBIOLOGY SOCIETY

OPEN ACCESS

VP24 matrix proteins of eight filoviruses downregulate innate immune response by inhibiting the interferon-induced pathway

Hira Khan[1,*], Lav Tripathi[1], Pekka Kolehmainen[1], Rickard Lundberg[1], Eda Altan[1], Jemna Heroum[1], Ilkka Julkunen[1,2], Laura Kakkola[1,†] and Moona Huttunen[1,†]

Abstract

Filoviruses encode viral protein 24 (VP24) which effectively inhibit the innate immune responses in infected cells. Here we systematically analysed the effects of nine mammalian filovirus VP24 proteins on interferon (IFN)-induced immune response. We transiently expressed Ebola, Bombali, Bundibugyo, Reston, Sudan and Taï Forest ebolavirus (EBOV, BOMV, BDBV, RESTV, SUDV, TAFV, respectively), Lloviu virus (LLOV), Mengla dianlovirus (MLAV) and Marburgvirus (MARV) VP24 proteins and analysed their ability to inhibit IFN-α-induced activation of myxovirus resistance protein 1 (MxA) and interferon-induced transmembrane protein 3 (IFITM3) promoters. In addition, we analysed the expression of endogenous MxA protein in filovirus VP24-expressing cells. Eight filovirus VP24 proteins, including the VP24s of the recently discovered MLAV, BOMV and LLOV, inhibited IFN-induced MxA and IFITM3 promoter activation. MARV VP24 was the only protein with no inhibitory effect on the activation of either promoter. Endogenous MxA protein expression was impaired in cells transiently expressing VP24s with the exception of MARV VP24. We mutated nuclear localization signal (NLS) of two highly pathogenic filoviruses (EBOV and SUDV) and two putatively non-pathogenic filoviruses (BOMV and RESTV), and showed that the inhibitory effect on IFN-induced expression of MxA was dependent on functional cluster 3 of VP24 nuclear localization signal. Our findings suggest that filovirus VP24 proteins are both genetically and functionally conserved, and that VP24 proteins of most filovirus species are capable of inhibiting IFN-induced antiviral gene expression thereby efficiently downregulating the host innate immune responses.

INTRODUCTION

Filoviridae is one of the eleven families of the order *Mononegavirales*. Family *Filoviridae* consists of six genera: *Ebolavirus*, *Marburgvirus*, *Cuevavirus*, *Dianlovirus*, *Striavirus*, and *Thamnovirus* [1, 2]. The genera *Cuevavirus*, *Striavirus Dianlovirus*, and *Thamnovirus* have one species each: *Lloviu cuevavirus* (Lloviu virus, LLOV), *Xilang striavirus* (Xilang virus, XILV), *Mengla dianlovirus* (Mengla virus, MLAV) and *Huángjio thamnovirus* (Huángjio virus, HUJV), respectively. *Marburg marburgvirus* (Marburg virus, MARV) and *Ravn marburgvirus* (Ravn virus, RAVV) are the two members of the *Marburgvirus* genus, whereas the *Ebolavirus* genus includes six species: *Zaire ebolavirus* (Ebola virus, EBOV), *Sudan ebolavirus* (Sudan virus, SUDV), *Taï Forest ebolavirus* (Taï Forest virus, TAFV), *Reston ebolavirus* (Reston virus, RESTV), *Bundibugyo ebolavirus* (Bundibugyo virus, BDBV), and *Bombali ebolavirus* (Bombali virus, BOMV) [3–5]. EBOV, SUDV, MARV, TAFV and BDBV are known to cause

Received 27 June 2023; Accepted 16 August 2023; Published 30 August 2023
Author affiliations: [1]Institute of Biomedicine, University of Turku, Kiinamyllynkatu 10, 20520 Turku, Finland; [2]Clinical Microbiology, Turku University Hospital, Kiinamyllynkatu 10, 20520 Turku, Finland.
***Correspondence:** Hira Khan, hira.khan@utu.fi
Keywords: filovirus; IFITM3; innate immunity; interferon; MxA; nuclear localization signal; VP24.
Abbreviations: BDBV, Bundibugyo virus; BOMV, Bombali virus; EBOV, Ebola virus; EVD, Ebolavirus disease; FBS, fetal bovine serum; GP/sGP, glycoprotein/secreted glycoprotein; HEK293, human embryonic kidney 293; Huh7, human hepatoma 7; HUJV, Huangio virus; IFITM3, interferon-induced transmembrane protein 3; IFN, interferon; IL-10R2, interleukin-10-receptor-2; IRF9, interferon regulatory factor 9; ISG, interferon-stimulated gene; ISGF3, interferon-stimulated gene factor 3; JAK, Janus kinase; LLOV, Lloviu virus; Luc, luciferase; MARV, Marburgvirus; MEM, Dulbecco's modified Eagle's medium; MLAV, Mengla dianlovirus; MxA, myxovirus resistance protein 1; MxB, myxovirus resistance protein 2; NLS, nuclear localization signal; NP, nucleoprotein; OAS, oligoadenylate synthetase; RAVV, Ravn virus; RESTV, Reston virus; RSV, Rous Sarcoma virus; STAT, signal transducer and activator of transcription; SUDV, Sudan virus; TAFV, Tai Forest virus; VP, viral protein; XILV, Xilang virus.
The data presented in this study are available on request from the corresponding author. The data is not publicly available due to the small size of produced data (e.g. alignment data of sequences). All of the VP24 sequences used for analysis in the study are available in the NCBI GenBank repository (https://www.ncbi.nlm.nih.gov/genbank/) under accession numbers listed in the methods section and Fig. S1.
†These authors contributed equally to this work
One supplementary figure is available with the online version of this article.

disease in humans, and especially EBOV, SUDV and MARV cause very severe and often fatal haemorrhagic fever disease. The largest Ebolavirus disease (EVD) outbreak occurred in the West African region in 2014–2015, with >28000 cases and >11000 deaths [6].

Virus infection activates innate immune responses that mediate early defence mechanisms of the cell against infection. Virus infection triggers signalling cascades leading to the production and secretion of interferons (IFNs), especially type I and type III IFNs (IFN-α/β and IFN-λ, respectively). Secreted IFNs bind to the cell surface receptors: type I IFNs to the IFNAR1 and IFNAR2, and type III to a heterodimeric receptor composed of the type III interferon receptor (IFNLR1) and interleukin-10-receptor-2 (IL-10R2). The binding of IFNs to their receptors leads to dimerization and phosphorylation of the receptor molecules leading to activation of the Janus kinase (JAK)–signal transducer and activator of transcription (STAT) pathway (JAK/STAT pathway) [7]. JAKs subsequently phosphorylate STAT1 and STAT2, which form a heterodimer that is translocated into the nucleus via importin-α/β transport system. In the nucleus STAT1-STAT2 complexes bind to IFN regulatory factor 9 (IRF9), generating a heterotrimeric transcription factor complex, IFN-stimulated gene factor 3 (ISGF3). ISGF3 complexes bind to IFN-stimulated response elements on the promoter areas of IFN-responsive target genes. The activation of promoters results in the transcription of interferon-stimulated genes (ISGs), and the production of a wide range of antiviral proteins, such as myxovirus resistance protein 1 (MxA), myxovirus resistance protein 2 (MxB), viperin, interferon-induced transmembrane protein 3 (IFITM3), 2',5'-oligoadenylate (2–5A) synthetase (OAS), and RNA activated protein kinase (PKR), that confer an antiviral state with several mechanisms both in infected and in bystander cells [8].

Filoviruses have evolved highly effective strategies to escape and/or delay innate immune response mechanisms of virus-infected cells. Filoviruses are non-segmented negative-stranded RNA viruses that encode seven to eight proteins: nucleoprotein (NP), viral protein (VP) 24, VP30, VP35, VP40, glycoprotein/secreted glycoprotein (GP/sGP), and RNA-dependent RNA polymerase (L) [9]. Of these proteins, especially VP24 and VP35 have been shown to perturb the activation of innate immune responses [10].

VP35 is a multifunctional protein, showing its main inhibitory effect on the induction of IFN production and dendritic cell maturation [11], whereas VP24 is considered the main inhibitor of the IFN-induced pathway. EBOV, BDBV, RESTV and LLOV VP24s have been shown to inhibit the IFN-induced signalling pathway [12–14]. The main mechanism of action is the ability of VP24 to bind with its nuclear localization signal (NLS) to importins and prevent the binding of activated phosphorylated STATs to importin, inhibiting the translocation of STAT complexes into the nucleus. In contrast to the four VP24s above, MARV and MLAV VP24s have not been shown to inhibit IFN-induced pathway [15, 16]. Although the mechanism of inhibition has been shown for EBOV, LLOV, BDBV and RESTV VP24s [12–14], the inhibitory effects of VP24s have not been studied in the same experimental settings, the effect of SUDV or TAFV VP24s has not been studied and the effect of recently discovered filovirus VP24 of BOMV is not known.

Here, we analysed the ability of nine filovirus VP24s to interfere with IFN-induced innate immune responses leading to the activation of IFN-regulated MxA and IFITM3 promoters. One filovirus VP24 (MARV) showed no inhibition, while the remaining eight VP24s (EBOV, BOMV, BDBV, RESTV, SUDV, TAFV, LLOV and MLAV), including the recently discovered BOMV, LLOV and MLAV, efficiently inhibited IFN-induced activation of MxA promoter and the production of endogenous MxA. IFITM3 promoter activation was efficiently inhibited by seven VP24s, while BDBV VP24 showed less and MARV no inhibitory effect. We showed the inhibitory effect to be dependent on the functional cluster three of nuclear localization signal of VP24s. Our findings provide new information on the effect of nine mammalian filovirus VP24s on the IFN-induced signalling pathway.

METHODS

Sequence comparison of VP24 proteins

Filovirus VP24 protein sequences were obtained from the GenBank (accession number for each sequence included in Fig. S1, available in the online version of this article), and aligned with ClustalW [17]. Maximum likelihood method coupled with general reverse transcriptase model was used for the analysis of the phylogenetic relationship of filovirus VP24 amino acid sequences in the MEGA11 platform. Evolutionary rate differences among sites were modelled using gamma distribution with allowance for some sites to be evolutionarily invariable. Evolutionary confidence was tested with 100 rounds of bootstrapping [18]. The structure of EBOV VP24 was created with Chimaera v1.15 based on 4M0Q (RCSP Protein Data Bank) VP24 as a model.

Cells and reagents

Human embryonic kidney (HEK293) and human hepatoma (Huh7) cells were maintained at 37 °C in a 5% CO_2 in Dulbecco's Modified Eagle's medium (MEM) (Lonza Biowhittaker), supplemented with HEPES (MP Biomedicals), 10% heat-inactivated fetal bovine or calf serum (FBS or Integro), 1% penicillin/streptomycin (Lonza Biowhittaker), and 1 x Glutamax (ThermoFischer Scientific).

Plasmids

VP24 sequences for EBOV (Genbank accession number KM233113), BOMV (Genbank accession number MF319185), BDBV (Genbank accession number KC545394), RESTV (Genbank accession number KY798006), SUDV (Genbank accession number KC545389), TAFV (Genbank accession number KU182910), LLOV (Genbank accession number NC016144.1), MARV (Genbank accession number KC545387.1) and MLAV Genbank accession number (KX371887) were obtained from GenBank and cloned by GeneArt (ThermoFischer Scientific) into expression vector pEBB-HA-N (kind gift from Professors Kalle Saksela and David Baltimore) that encodes proteins with an N-terminal HA-tag. Due to the low expression of the original genes, codon-optimized VP24 genes of BDBV and MARV were synthesized and cloned into the expression plasmid pEBB-HA-N by GeneArt (ThermoFischer Scientific). The putative nuclear localization signals (NLS) of BOMV, RESTV and SUDV VP24s were mutated as EBOV VP24 was previously [19].

For reporter gene assays, MxA promoter in front of a firefly luciferase gene (MxA-Luc) [13] and Renilla luciferase gene under Rous Sarcoma virus promoter (RSV-Renilla) were used. The human IFITM3 promoter was constructed by taking 600 bases upstream region of IFITM3 translation start site (Genbank accession number NM_021034.3) using the thirteenth patch release for the human GRCh38 reference assembly (GRCh38.p13). The sequence was inserted upstream of the luciferase gene into the pGL4.11 vector (IFITM3-Luc). For protein expression in *E. coli*, the IFITM3 gene (Genbank accession number NM_021034.2) was cloned into pGEX-2T vector.

IFITM3 and MxA antibody production

N-terminally GST-tagged IFITM3 protein was expressed in *E. coli* (BL21 strain) and purified from inclusion bodies under denaturing conditions with preparative SDS-PAGE (Biorad). The pooled fractions were concentrated with Amicon filters (10 KDa MWCO) and analysed on SDS-PAGE. Rabbits and guinea pigs were immunized with three doses (50 µg/dose) of purified GST-IFITM3 protein at 2 week intervals using Freund's complete (first dose) and incomplete (second and third doses) adjuvants. Sera were collected 10 days post-immunizations and analysed for the presence of IFITM3-specific antibodies with immunoblotting. MxA protein production in the baculovirus system and rabbit anti-MxA antibody production have been described before [20]. Guinea pigs were immunized as above with three doses (50 µg/dose) of baculovirus-produced MxA [20] followed by bleeding 10 days after the last immunization. Sera were analysed for the presence of MxA-specific antibodies with immunoblotting.

Transfections and cell inductions

TransIT-LT1 (Mirus Bio LCC) reagent was used to transfect plasmids into HEK293 and Huh7 cells according to the manufacturer's instructions. The interferon-induced pathway was induced by supplementing cell culture media with peginterferon alfa-2a (IFN-α–2a; Pegasys, F. Hoffman-La Roche) at a concentration of 10 ng ml^{-1}. Huh7 cells were used for immunofluorescence due to their big size and clearly visible cytoplasm and nucleus. HEK293 cells were used for the luciferase assays and importin binding experiments due to the high transfection efficiency. The expression levels of proteins were analysed in both cell lines.

Immunoblotting

To assess protein expression levels, HEK293 and Huh7 cells on 12-well plates were transfected with 1200–1500 ng/well of VP24 expression plasmids. After overnight incubation, the cells were lysed on ice with a native lysis buffer composed of 50 mM Tris-HCl, 150 mM NaCl, 1 mM EDTA and 1% NP40 supplemented with a complete protease inhibitor cocktail (F. Hoffman-La Roche), and Pierce Universal Nuclease (Rockford). Proteins were separated on 10% SDS-PAGE and transferred to PVDF blotting membranes (Amersham, Merck KGaA) with a wet transfer system. Expressed VP24s were detected with mouse anti-HA1.1 epitope tag (1:1000) (BioLegend), and GADPH protein was detected with mouse anti-GAPDH (1:700) (6C5, Santa Cruz Biotechnology) as a loading control. Primary antibodies were detected with IRDye 680RD goat anti-mouse IgG (1:15000) (LI-COR Biosciences), and the membranes were scanned and images were captured with Odyssey Fc Imaging system (LI-COR Biosciences).

To determine the endogenous expression levels of MxA and IFITM3 proteins upon IFN induction, Huh7 cells were induced with different doses of IFN-α–2a on 12-well plates. Cell lysates were collected and proteins were separated as above. Proteins were transferred to nitrocellulose blotting membrane (Amersham, Merck KGaA) with a semi-dry transfer system. Endogenous MxA and IFITM3 proteins were detected with in-house rabbit anti-MxA antibody (1:1000) [20] and in-house rabbit anti-IFITM3 antibody (1:1000). Mouse anti-GAPDH (1:700) (6C5, Santa Cruz Biotechnology) was used for GAPDH as a loading control. Primary antibodies were detected with IRDye 800RD goat anti-rabbit IgG (1:15000) and IRDye 680RD goat anti-mouse IgG (1:15000) (LI-COR Biosciences) and the membranes were scanned and imaged as above.

Importin binding assay

The importin binding capacity of BOMV, RESTV and SUDV VP24s was analysed as described before with some modifications (21). Briefly, GST and human GST-importin α5 were produced in *E. coli* (BL21), and induced with 0.5 mM IPTG for 4 h at 37 °C, the induced cells were lysed with lysis buffer (20 mM Tris-Cl, pH 8, 150 mM NaCl, 1 mM $MgCl_2$, 5% glycerol, 0.2% Triton X100,

250 µg ml^{-1} lysozyme and protease inhibitor). The *E. coli* cells were kept on ice for 30 min, and 20 s ON / 20 s OFF sonication cycle was carried out for a total of 8 min. The supernatant was separated by centrifugation and proteins were quantified by Western blotting. Equal amount of GST and GST-importin-α5 were allowed to bind to Glutathione Sepharose 4B beads (GE Healthcare) at room temperature for 1 h, followed by washing steps. Lysates of VP24 expressing HEK293 cells (24 h post-transfection) were allowed to bind to Sepharose-immobilized GST or GST-importin α5 at 4 °C overnight. The binding of HA-tagged VP24s was analysed by immunoblotting.

Luciferase reporter gene assays

Dual luciferase assays were used as described previously [8, 21]. Briefly, HEK293 cells were transfected on 96-well plates with promoter-luciferase constructs (20 ng/well) and VP24 expression plasmids (3–30 ng/well). RSV-Renilla (50 ng/well) was used as an internal transfection efficacy control. After overnight incubation, the cells were stimulated with 10 ng ml^{-1} of IFN-α–2a for 20–24 h. For the Twinlite Firefly and Renilla Reporter Gene Assay System (Perkin Elmer), cells were harvested according to the manufacturer's recommendations. The luminescence was measured with Victor Nivo Multi-mode Plate Reader (Perkin Elmer) and the Renilla luciferase levels were utilized to normalize the firefly luciferase data. Every experiment was performed in triplicates and repeated at least three times, and figures were compiled of the two representative experiments (n=6 for each bar).

Immunofluorescence

Huh7 cells were seeded on 96-well plates or on 12-well or 6-well plates with coverslips. Following 20–24 h of transfection with N-terminally HA-tagged VP24 expression plasmids, cells were induced with 10 ng ml^{-1} IFN-α–2a overnight. The cells were fixed with 4% paraformaldehyde at room temperature for 15–20 min, blocked and permeabilized with 5% BSA and 0.1% Triton-X 100 in PBS at room temperature for 30 min. For MxA experiments cells were permeabilized for 5 min after fixing. Cells were incubated for 1 h at room temperature with mouse anti-HA 1.1 Epitope tag (1:1000) (BioLegend) and an in-house anti-MxA antibody pool raised in three guinea pigs (1:16000) diluted in 3 or 5% BSA/PBS. Following BSA/PBS washes, the cells were labelled for 1 h at room temperature with Alexa Fluor 568 goat anti-mouse and Alexa Fluor 488 goat anti-guinea pig antibodies (Invitrogen, Thermo Fisher Scientific). Coverslips were mounted on objective slides using mounting media containing DAPI (Invitrogen). On 96-well plates, the nuclei were stained with DAPI (1:2500) (Thermo Fisher Scientific) diluted in 5% BSA/PBS. The cells on 96-well plates were imaged with an Evos microscope with a 20× objective (Thermo Fisher Scientific). The coverslips were imaged using DFC7000 T fluorescent microscope (Leica) or SP8 Falcon confocal microscope (Leica) with a 63× objective. The images were manually quantified with Image J software.

Statistical analysis

GraphPad Prism version 9.2.0 for Windows (GraphPad Software), was used to determine the statistically significant differences for the luciferase assay results using ordinary one-way ANOVA Dunnett's multiple comparisons test with a single pooled variance. For the VP24 nuclear localization and the MxA localization statistical analysis unpaired, non-parametric, two-tailed, Mann-Whitney tests were performed.

RESULTS

Filovirus VP24 sequence comparison

We have previously shown that VP24 amino acid sequences of the virus species belonging to the genus *Ebolavirus* (EBOV, BOMV, TAFV, RESTV, SUDV and BDBV) are very similar (identity 74–90%), whereas LLOV, MARV, and MLAV differ from the genus *Ebolavirus* (identities to EBOV VP24 59, 36 and 38%, respectively) [21]. To analyse the amino acid sequence variation at the VP24 region within filovirus species, altogether 112 filovirus isolates from the years 1967–2021 were compared (Table 1, Fig. S1). Strikingly, within the filovirus species only up to six amino acid changes were identified among the 250–253 amino acid regions of all analysed VP24s. The most variable sequences were the 20 isolates of RESTV collected in the years 1989–2018 and the 20 isolates of MARV collected in the years 1967–2012, showing 0–6 and 0–5 amino acid changes, respectively. For MLAV only one sequence has been deposited into the GenBank thereby not allowing sequence comparison within the species. Other species showed less variation than RESTV and MARV, e.g. twenty EBOV isolates from the years 1967–2021 showed only 0–2 amino acid changes in their VP24 sequences. Overall, the VP24 amino acid sequence is stable within the species and amino acid mutations do not seem to occur frequently. Thus, one VP24 sequence of a representative strain likely functionally represents each filovirus species.

The amino acid changes of Zaire ebolavirus (EBOV), Bombali ebolavirus (BOMV), Bundibugyo ebolavirus (BDBV), Mengla dianlovirus (MLAV), Reston ebolavirus (RESTV), Sudan ebolavirus (SUDV), Taï Forest ebolavirus (TAFV), Lloviu cuevavirus (LLOV) and Marburg marburgvirus (MARV) are shown as numbers and as percentages of amino acid changes compared within species between different years.

The nuclear localization signal (NLS), especially the cluster 3 of NLS [12], is important in the function of EBOV VP24. Alignment of cluster 3 NLS of the nine filovirus VP24s used in this study (Fig. 1) shows no amino acid differences in BOMV, BDBV and

Table 1. Comparison of VP24 amino acid sequences of 112 filovirus isolates representing nine filovirus species

Species	no. of sequences	Collection years	no. of amino acid changes in VP24	Amino acid change %
EBOV	20	1976–2021	0–2	0–0.8
BOMV	8	2016–2019	0–1	0–0.4
BDBV	20	2007–2012	0–2	0–0.8
MLAV	1	2015	0	0
RESTV	20	1989–2018	0–6	0–2.4
SUDV	20	1976–2012	0–2	0–0.8
TAFV	1	1994	0	0
LLOV	2	2003–2019	0–3	0–1.2
MARV	20	1967–2012	0–5	0–2.0

TAFV compared to EBOV, and only one amino acid difference (L or Q ->V, marked in pink in Fig. 1) in RESTV, SUDV and LLOV, whereas MLAV and MARV sequences differ considerably from that of EBOV.

Filovirus VP24 expression in HEK293 and Huh7 cells

Representative VP24s of the nine filoviruses were cloned for expression in mammalian cells. In addition, the cluster 3 of the putative nuclear localization signal in VP24s of EBOV, BOMV, RESTV and SUDV was mutated, resulting in full-length NLS-mutated

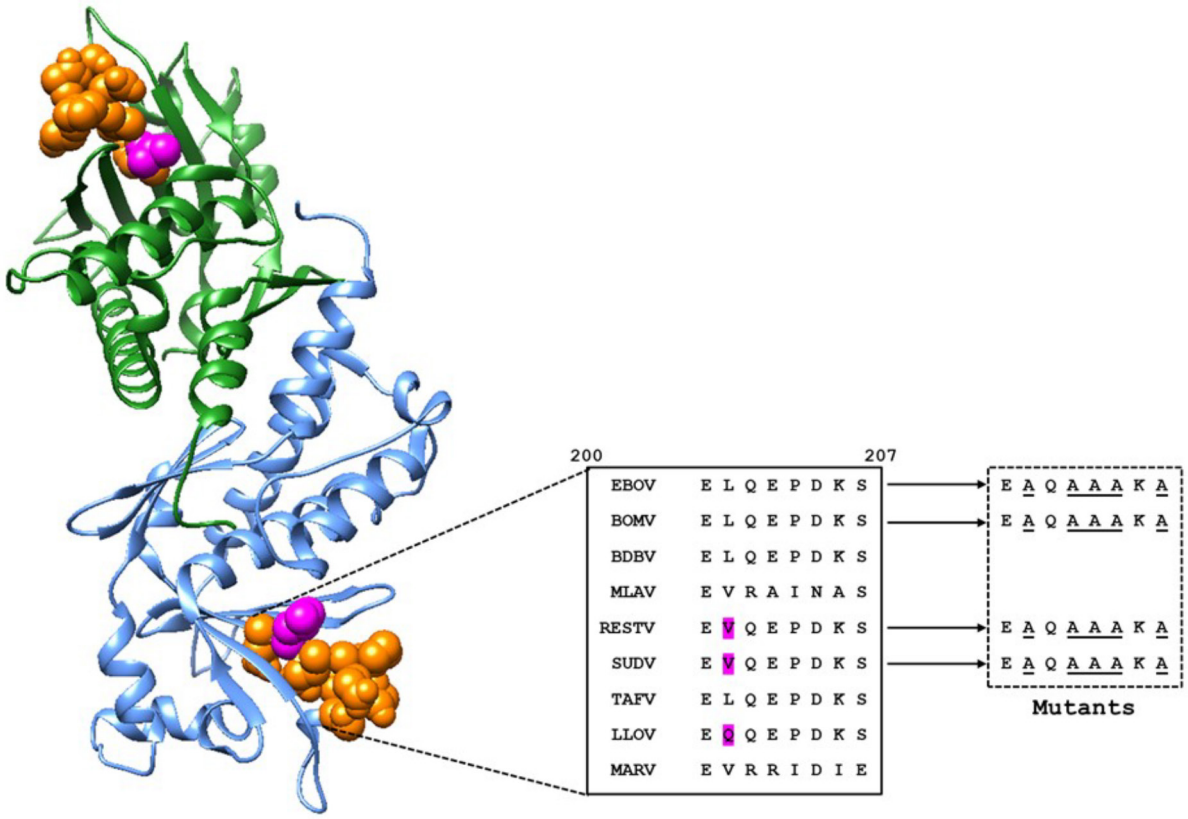

Fig. 1. Structure of EBOV VP24 dimer (green and blue ribbons). Nuclear localization signal of VP24 is shown as orange spheres, where the pink spheres indicate the single amino acids of RESTV, SUDV and LLOV differing from EBOV. Cluster three nuclear localization signal of each nine filovirus VP24s is aligned (pink boxes correspond to pink spheres) and the introduced mutations to alanine residues are indicated.

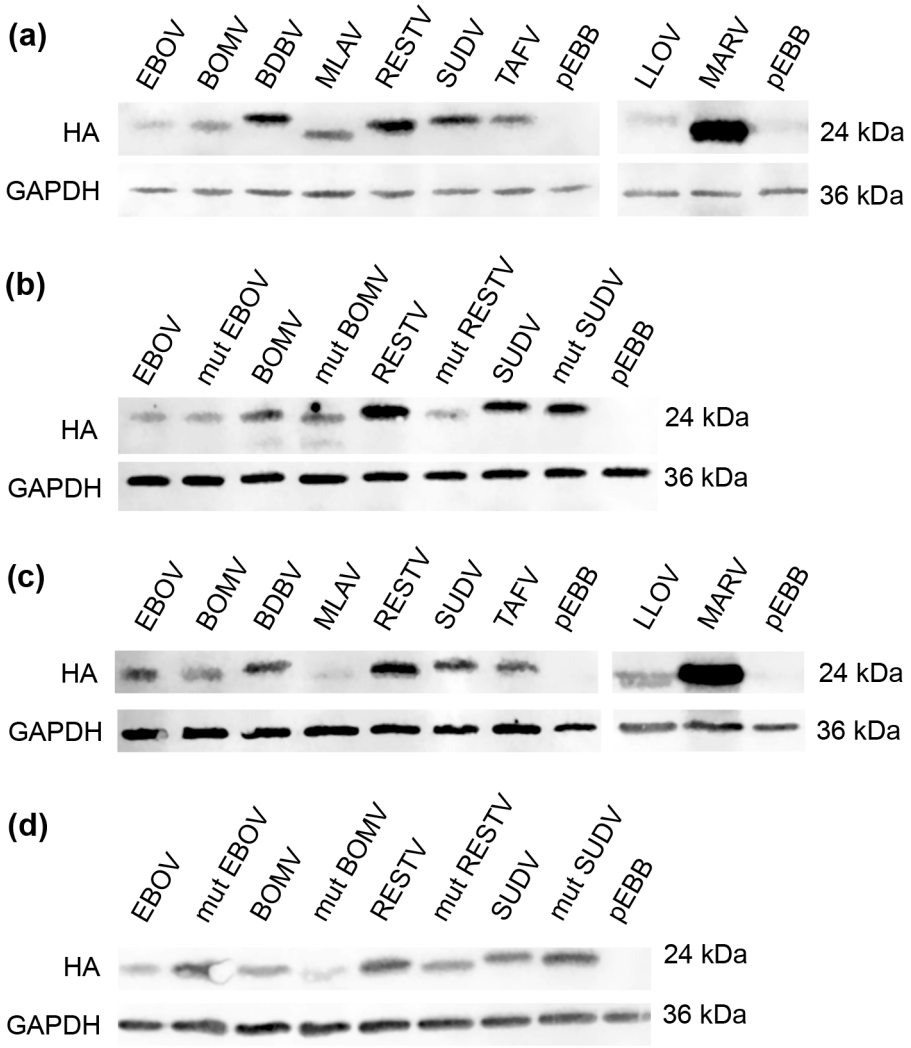

Fig. 2. Expression of N-terminally HA-tagged VP24 and NLS-mutated VP24 proteins in HEK293 (a and b) and Huh7 (c and d) cells. Empty vector-transfected (pEBB) cells were used as a control; GAPDH was used as a loading control.

VP24s (amino acid changes to alanine are shown in Fig. 1). The selected four NLS-mutants represent the two main sequences of cluster 3, and include highly pathogenic and potentially non-pathogenic filoviruses, as also the recently discovered BOMV. To verify the expression of nine filovirus VP24 proteins and the four NLS-mutated VP24s in HEK293 and Huh7 cells, cell lysates from transfected cells were analysed with immunoblotting (Fig. 2). Empty vector-transfected (pEBB) cells were used as controls, and GAPDH was detected as a loading control. All nine VP24s and all four NLS-mutated VP24s were readily expressed in both HEK293 (Fig. 2a, b) and Huh7 (Fig. 2c, d) cells. The expression of the original BDBV and MARV VP24 sequences was inefficient (not shown), whereas the codon-optimized VP24s of BDBV and MARV were readily expressed (Fig. 2). The codon-optimized constructs of BDBV and MARV were used in subsequent experiments.

Nuclear localization and importin binding of NLS-mutated VP24s

To study the function of cluster 3 of NLS of EBOV, SUDV, BOMV and RESTV VP24s, the nuclear localization of the NLS-mutated VP24s was analysed in transfected Huh7 cells with immunofluorescence (Fig. 3). The wild-type VP24s of EBOV, SUDV, RESTV and the recently discovered BOMV were readily expressed and localized predominately into the nuclei, whereas the NLS-mutated VP24s localized either in the cytoplasm or diffusively in the cytoplasm and nuclei (Fig. 3a). Quantification of the nucleus localized VP24s clearly shows that the mutation of cluster three amino acids on EBOV, BOMV, RESTV and SUDV NLSs significantly reduces the nuclear accumulation of these VP24s (Fig. 3b).

To analyse if the NLS-mutated VP24s were devoid of nuclear accumulation due to impaired binding to importin, the wild-type and NLS-mutated VP24s of EBOV, BOMV, RESTV and SUDV were allowed to bind to importin α5, and the bound VP24 was

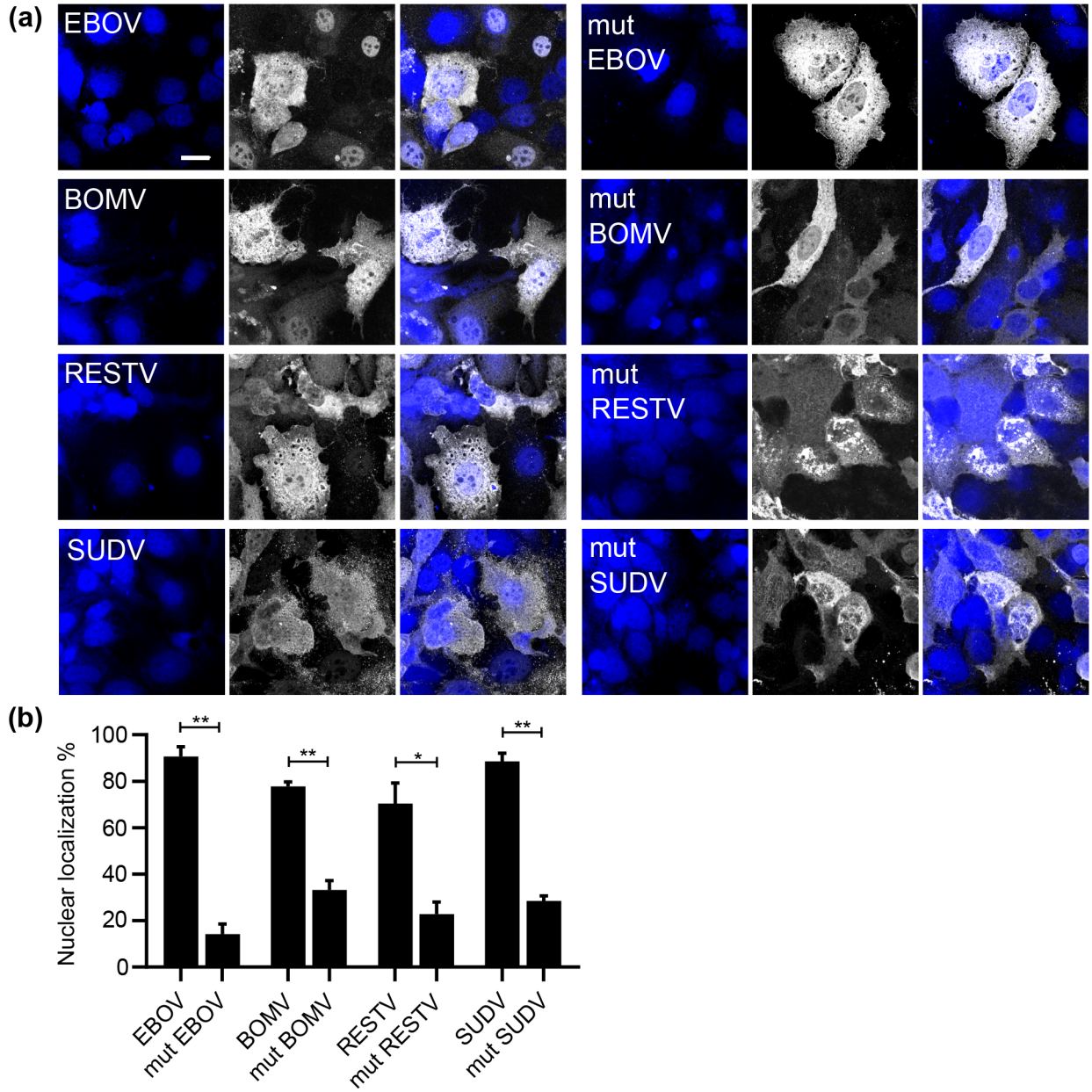

Fig. 3. Nuclear localization of NLS-mutated VP24s. (a) The subcellular localization of four NLS-mutated VP24s (EBOV, BOMV, RESTV, SUDV) and the respective wild-type VP24s was analysed by immunofluorescence in transfected Huh7 cells. Cells were labelled with anti-HA (staining HA-tagged VP24s, white) and nuclei were stained with DAPI (blue). (b) Nuclear localization of VP24s and NLS-mutated VP24s was quantified from the immunofluorescence pictures. A total of 150 cells from three replicates were quantified. Each bar shows the averages of three biological experiments. Error bars represent the standard error of the means. *P* values were calculated using unpaired, non-parametric, two-tailed, Mann-Whitney test, $^{**}p < 0.01$; $^{*}p < 0.05$. Scale bar 10 µm.

detected with immunoblotting (Fig. 4a). As in our previous study [21], EBOV VP24 bound strongly to importin α5 and the mutation of NLS reduced this binding (Fig. 4a, b). MARV VP24 was used as control, and as expected, it did not bind importin α5 (Fig. 4c). Despite some unspecific binding to GST alone, BOMV, RESTV and SUDV VP24s showed similar binding tendency as EBOV VP24, with NLS mutation reducing binding to importin α5. VP24 of the recently discovered BOMV, with cluster three identical to EBOV, bound to importin α5 and showed a clear reduction in binding of NLS-mutated VP24 (Fig. 4b). Regardless of the differences in binding capacities to importin α5, these results indicate that the cluster three area is an active NLS in the four analysed VP24s and responsible for the nuclear accumulation of VP24s.

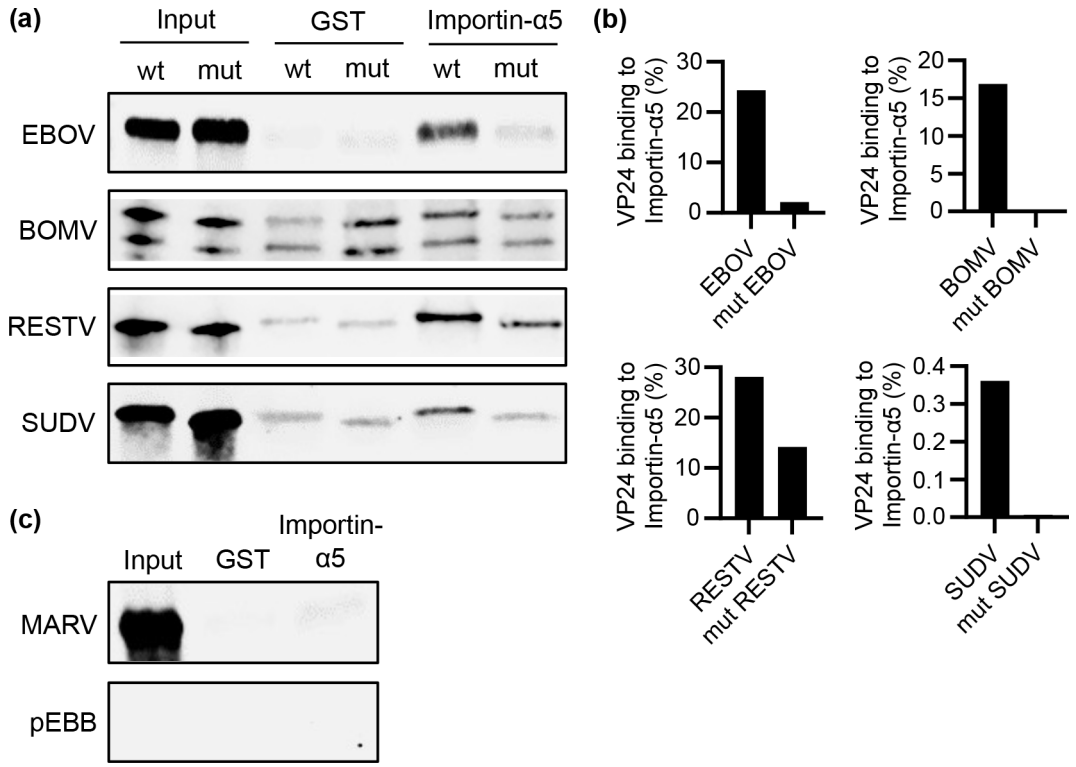

Fig. 4. Binding of VP24s to importin α5. (a) Wild-type and NLS-mutated VP24s of EBOV, BOMV, RESTV, and SUDV were expressed in HEK293 cells. Cell lysates were allowed to bind to immobilized importin α5, and bound VP24s were detected with immunoblotting. (b) Quantification of the bound VP24 was analysed by comparing the band intensities of bound VP24s to the corresponding input. The unspecific binding to GST was deducted from signal intensities. (c) MARV VP24 was used as a control. Input represents 1/10 of the input sample used for importin α5 binding.

Induction of MxA and IFITM3 with interferon

IFN induces the signalling pathway leading to the activation of MxA and IFITM3 promoters and the expression of respective IFN-induced antiviral proteins. To establish an optimal concentration of IFN-α–2a for the production of MxA and IFITM3 proteins, Huh7 cells were stimulated overnight with increasing doses of IFN-α–2a followed by an analysis of expression of MxA and IFITM3 proteins by immunoblotting (MxA in Fig. 5a and IFITM3 in Fig. 5b). Uninduced cells (MOCK) show the basal expression levels of MxA and IFITM3. As shown in Fig. 5, increasing the concentration of IFN-α–2a resulted in increased expression levels of MxA and IFITM3. The expression levels peaked at 3–10 ng ml^{-1} and at the highest IFN-α–2a concentration (30 ng ml^{-1}) there was no further increase in the expression levels of MxA or IFITM3 proteins. The basal expression level of MxA was not detectable, whereas the basal expression level of IFITM3 was clearly visible. For the subsequent immunofluorescence experiments, the IFN-α–2a concentration of 10 ng ml^{-1} was chosen to assess the effect of VP24s on IFN-induced MxA expression levels. Due to the constitutive expression of IFITM3, the effect of VP24s on IFN-induced IFITM3 protein expression was not analysed.

To optimize the amount of MxA and IFITM3 promoter-luciferase constructs for the reporter gene assays, MxA and IFITM3 promoter-luciferase constructs were transfected into HEK293 cells in increasing amounts (Fig. 5c, d). Transfected cells were stimulated with IFN-α–2a (10 ng ml^{-1}) for 20–24 h and cells were harvested for the luciferase assay. As shown in Fig. 5, increasing amounts of MxA and IFITM3 promoter-luciferase constructs led to increased activation of the promoters. To operate on the dynamic range of the assay, 20 ng of both MxA and IFITM3 promoter-luciferase constructs per well on a 96-well plate format were chosen for the subsequent reporter gene assays.

Eight filovirus VP24s inhibit the activation of MxA and IFITM3 promoters

In previous studies, EBOV, RESTV, BDBV and LLOV, but not MARV and MLAV, VP24s have been shown to inhibit IFN signalling [12–16, 22], whereas the effect of BOMV, SUDV or TAFV VP24s has not been studied. To study the effect of these nine mammalian filovirus VP24s, including the three recently discovered filoviruses, on IFN-induced pathway in the same experimental settings, HEK293 cells were co-transfected with expression plasmids for VP24 proteins and MxA or IFITM3 promoter-luciferase constructs. Transfected cells were stimulated with IFN-α–2a (10 ng ml^{-1}) overnight and luminescence activity was analysed with luciferase reporter gene assay. As shown in Fig. 6a, in the absence of any VP24 protein (empty vector

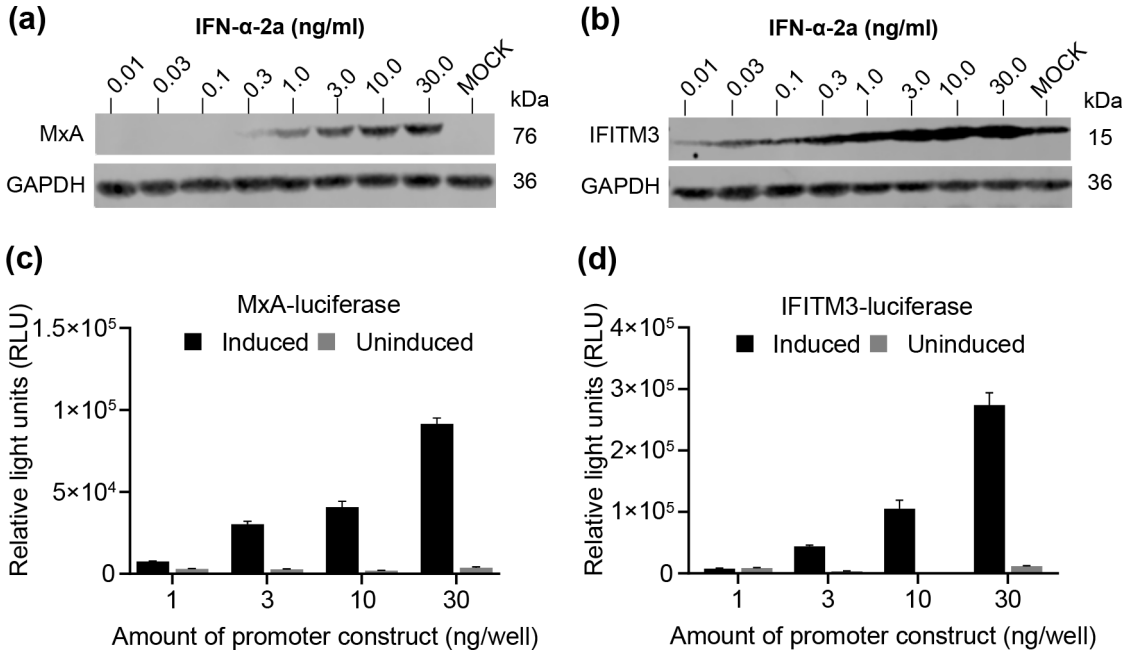

Fig. 5. Expression of IFN-α–2a induced endogenous MxA (a) and IFITM3 (b) proteins in Huh7 cells. Uninduced (MOCK) cells demonstrate the basal level of expression. Reporter gene assays for the activation of MxA (c) and IFITM3 (d) promoters (increasing amounts of expression plasmids) with IFN-α–2a induction (10 ng ml^{-1}) in HEK293 cells. Relative light units (RLUs) obtained from uninduced and IFN-α–2a-induced experiments are shown. Each bar shows the averages of two biological experiments with three technical replicates (*n*=6). Error bars represent the standard error of the means.

transfected cells; pEBB) IFN-induced cells showed high levels of MxA promoter activation. Eight filovirus VP24s (EBOV, BOMV, BDBV, MLAV, RESTV, SUDV, TAFV and LLOV) dose-dependently inhibited the MxA promoter activation, whereas MARV VP24 had no inhibitory effect on IFN-induced activation of MxA promoter (Fig. 6a). NLS mutated VP24s of EBOV, BOMV, RESTV and SUDV, with impaired ability to bind to importins, had no inhibitory effect on IFN-induced MxA promoter activation (Fig. 6b). The difference compared the wild-type VP24s to the respective NLS-mutated VP24s was significant, indicating that the importin binding capacity is essential for the inhibitory effect of VP24s. The inhibition of IFN-induced activation of IFITM3-promoter showed similar results, with eight filovirus VP24s dose-dependently inhibiting the activation, however, the inhibition by BDBV was not statistically significant (Fig. 6c). MARV VP24 and NLS-mutated VP24s (Fig. 6d) showed no or very weak inhibitory effect on the activation of IFITM3 promoter. In summary, eight filovirus VP24s were able to inhibit, with different levels of inhibition, IFN-induced activation of both MxA and IFITM3 promoters, and this inhibition was dependent on functional importin binding NLS.

Eight filovirus VP24s reduce the IFN-induced levels of endogenous MxA in Huh7 cells

To determine the effect of nine filovirus VP24s on the expression of IFN-induced endogenous MxA protein, VP24-expressing IFN-induced cells were analysed for MxA protein levels. To visualize the effect of filovirus VP24s on intracellular MxA, Huh7 cells were transfected with VP24 expression plasmids and stimulated with IFN-α–2a (10 ng ml^{-1}) for 24 h to allow sufficient time for MxA protein synthesis. MxA and VP24 proteins in cells were labelled with anti-MxA and anti-HA antibodies, respectively, immunofluorescence samples were imaged, and the expression status of MxA protein in VP24 expressing cells was quantified. As shown in Fig. 7, empty expression vector-transfected and uninduced Huh7 cells expressed undetectable levels of MxA (Fig. 7a; uninduced, pEBB), whereas empty expression vector-transfected and IFN-α–2a-induced cells (Fig. 7a; IFN-α–2a induced, pEBB) expressed high levels of MxA in the cell cytoplasm. The expression levels and subcellular localizations of VP24s were similar as qualified and quantified previously (Fig. 7a and [19, 21]) and on an average 90% of empty expression vector-transfected and IFN-α–2a-induced cells expressed MxA (Fig. 7b; dashed line). Upon expression of filovirus VP24 proteins, followed by IFN-induction, eight filovirus VP24s (EBOV, BOMV, BDBV, MLAV, RESTV, SUDV, TAFV and LLOV) clearly reduced the number of cells expressing endogenous MxA protein, whereas cells expressing MARV VP24 showed IFN-induced expression of MxA protein. These results confirm that in the VP24 expressing cells the inhibition of activation of MxA-promotor by eight VP24s also results in inhibition of endogenous MxA protein production.

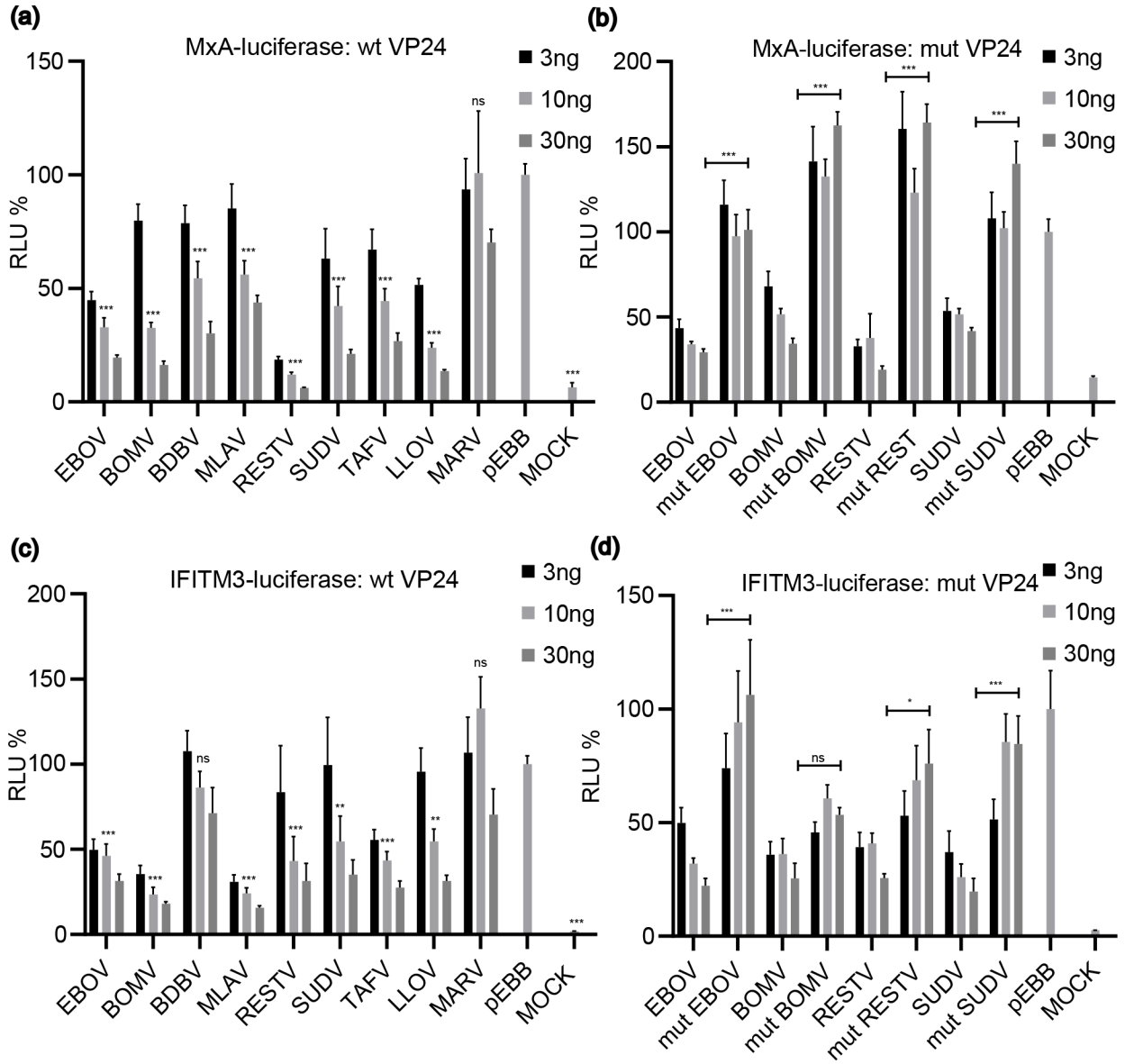

Fig. 6. Inhibitory effects of nine filovirus VP24s and NLS-mutated EBOV, BOMV, RESTV and SUDV VP24s on IFN-α–2a induced MxA (a, b) and IFITM3 (c, d) promoter activation. Empty expression plasmid transfected, IFN-α–2a induced cells (pEBB-HA) were used as a positive control and non-transfected cells (MOCK) as a negative control. Different colours in the bars refer to increasing amounts of VP24 expression plasmids (3, 10 or 30 ng). Each bar shows the averages of two biological experiments with three technical replicates (n=6). Error bars represent the standard error of the means. RLU values are normalized against pEBB (pEBB=100%). In graphs a and b statistical significances were calculated pairwise, comparing pEBB-control to individual VP24 expression plasmids (10 ng). In graphs b and d statistical significances were calculated pairwise, comparing wt VP24s to corresponding mutant form (30 ng). P values were calculated using ordinary one-way ANOVA Dunnett's multiple comparisons test with a single pooled variance, *p < 0.05, **p = < 0.0005, ***p = < 0.0001, ns=not significant.

Functional cluster 3 NLS is required for the inhibitory function of VP24s

To further verify the role of cluster three in VP24 NLS in the inhibitory effect of VP24s on IFN-induced expression of MxA protein, Huh7 cells were transfected with NLS-mutated VP24s of EBOV, BOMV, RESTV and SUDV, and MxA protein production was induced with IFN-α–2a (10 ng ml^{-1}). Immunofluorescence analysis was done as described above. As shown in Fig. 8, a mutation of NLS in any of the four filovirus VP24s results in marked IFN-induced expression of MxA in mutVP24-expressing cells (Fig. 8a). The difference is significant when comparing the positivity for IFN-induced MxA in VP24 expressing cells to NLS-mutated VP24 expressing cells (Fig. 8b). Altogether, these results indicate that the inhibitory effect of eight filovirus VP24s on IFN-induced expression of MxA depends on a functional cluster 3 NLS.

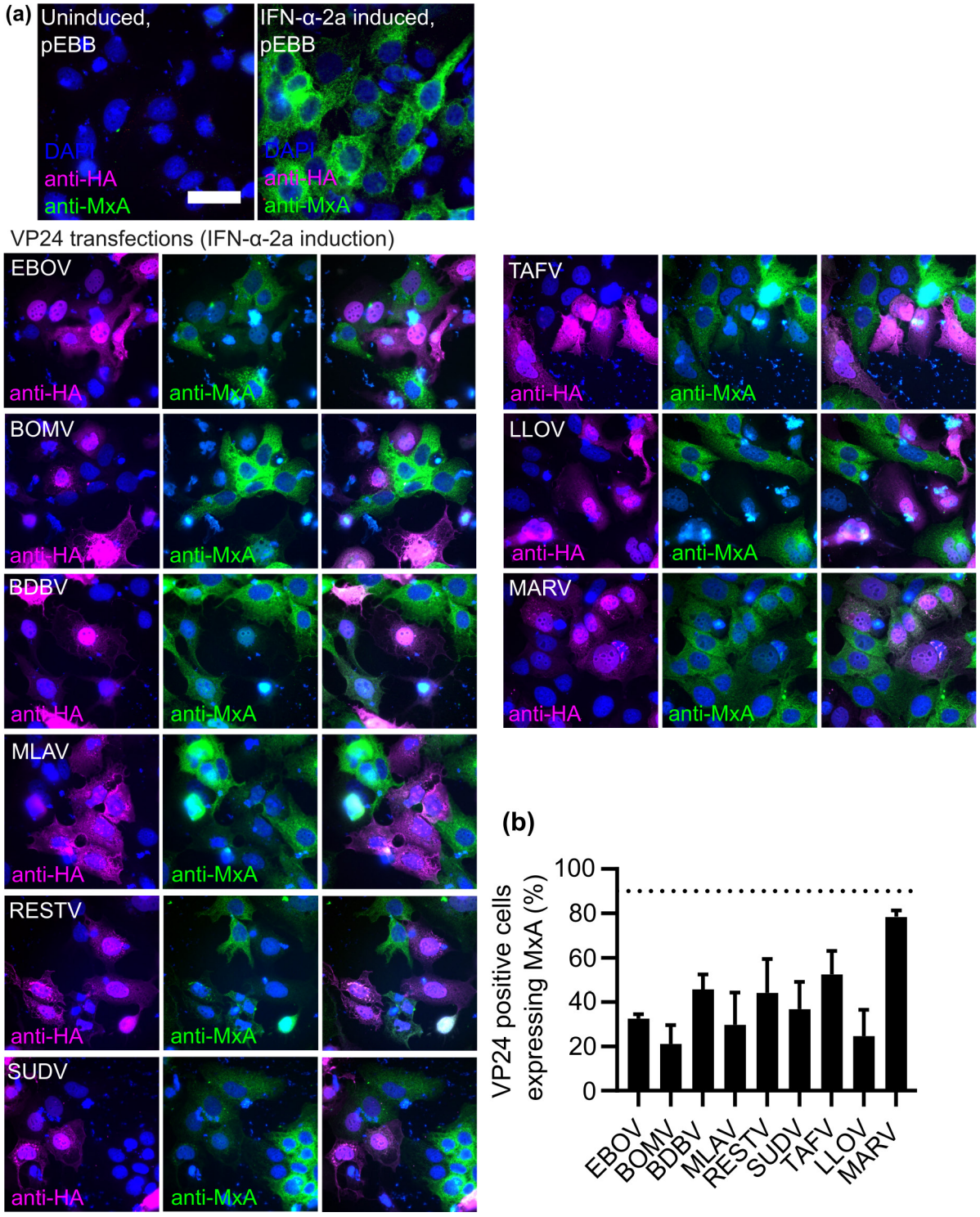

Fig. 7. Inhibitory effects of filovirus VP24s on IFN-α–2a induced MxA protein expression. (a) Representative immunofluorescence images of empty expression plasmid (pEBB) transfected uninduced and IFN-α–2a-induced Huh7 cells, and IFN-α–2a-induced Huh7 cells expressing filovirus VP24s. Cells were labelled with anti-HA (staining HA-tagged VP24s, magenta) and anti-MxA (staining endogenous MxA, green) antibodies. Nuclei were stained with DAPI (blue). Scale bar 20 µm. (b) Quantification of VP24 expressing, IFN-α–2a-induced, Huh7 cells positive for endogenous MxA. The analysis was repeated twice and for each VP24 ca. 200–300 VP24 positive cells we scored for the presence or absence of MxA expression. The dashed line indicates the average percentage of MxA positive Huh7 cells after IFN-α–2a induction (empty expression vector transfected).

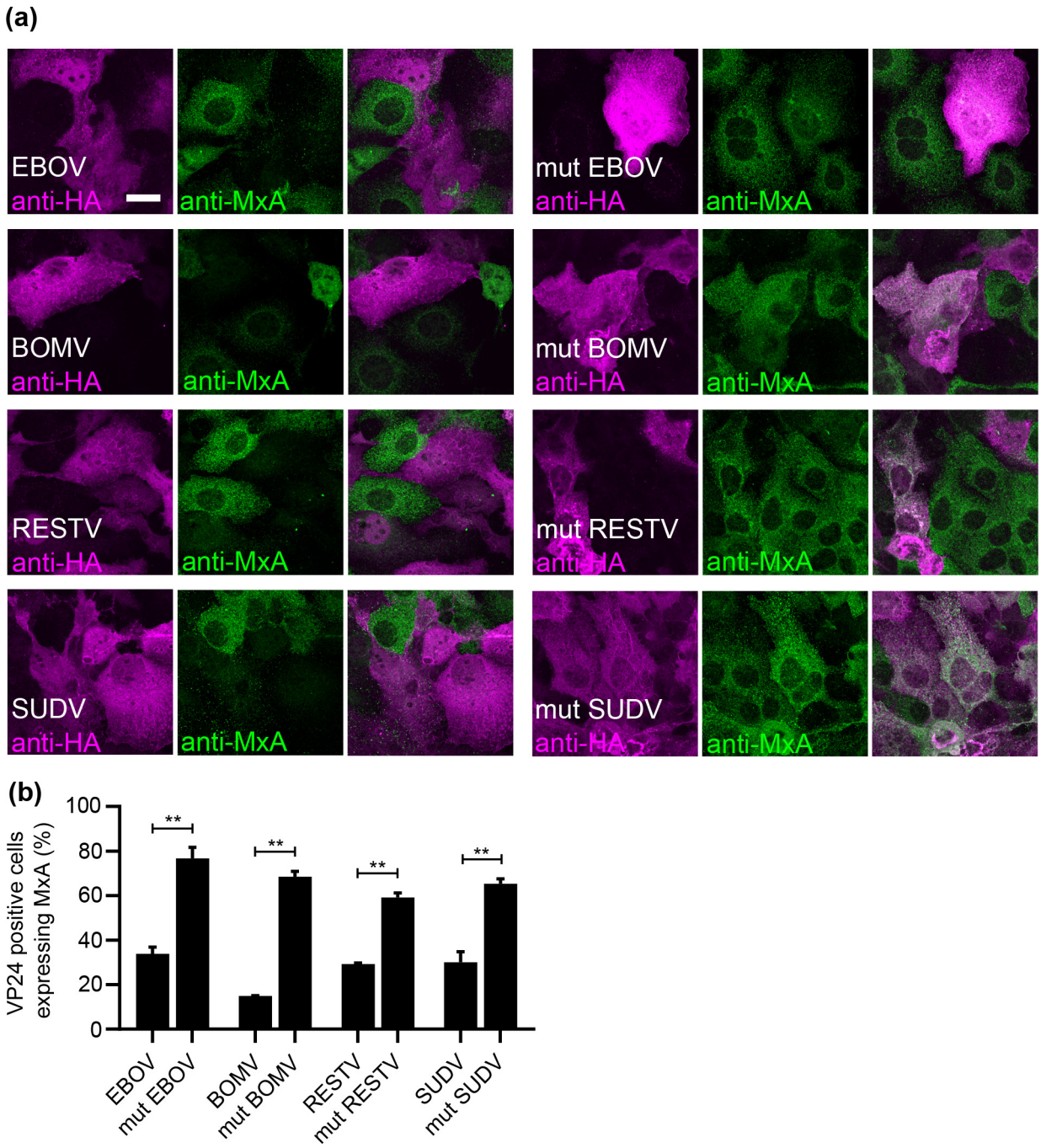

Fig. 8. The role of functional NLS on the inhibitory effect of VP24s. (a) Representative immunofluorescence images of VP24 and NLS-mutated VP24 transfected and IFN-α–2a-induced Huh7 cells. Cells were labelled with anti-HA (staining HA-tagged VP24s, magenta) and anti-MxA (staining endogenous MxA, green) antibodies. The white colour indicates the colocalization of VP24 and MxA protein. Scale bar 20 µm. (b) Quantification of VP24 expressing (wild-type or NLS-mutant), IFN-α–2a-induced, Huh7 cells positive for endogenous MxA. The analysis was repeated twice and for each VP24, ca. 200 VP24 positive cells we scored for the presence or absence of MxA expression. Error bars represent the standard error of the means. *P* values were calculated using unpaired, non-parametric, two-tailed, Mann-Whitney test, $^{**}p < 0.01$. Scale bar 10 µm.

DISCUSSION

Five species of filoviruses (EBOV, SUDV, TAFV, BDBV, MARV) are known to cause diseases in humans. Previously, unidentified filoviruses with unknown pathogenicity to humans are being discovered from animal reservoirs, such as LLOV in 2011 [23], BOMV in 2018 [24] and MLAV in 2019 [25], and these viruses can infect human cells but there are no identified human cases

to date. Filoviruses are zoonotic viruses, and spillover transmission to humans could lead to amino acid changes enabling these viruses to infect and spread in the human population. Evasion of immune responses is an important phenomenon during a virus life cycle, and especially VP24 protein seemed to accumulate amino acid changes during filoviral adaption to rodents [26]. The recent EBOV outbreaks and the newly discovered filoviruses emphasize the need for a better understanding of filovirus host cell interactions and the possible differences and similarities of the functions of viral proteins. In the present study, we have examined the effect of nine filovirus VP24 proteins on IFN-induced innate immune signalling pathway in cell models of human origin.

To assess the inhibitory potential of nine filovirus VP24s, we analysed their effect on IFN-induced pathway leading to activation of MxA and IFITM3 promoters and expression of endogenous MxA protein. MxA protein is an IFN-induced GTPase that exerts antiviral effects on many DNA and RNA viruses by targeting viral nucleocapsid structures and inhibiting the replication or transcription of the viruses [27]. IFITM3 is an IFN-inducible transmembrane protein found in endocytic vesicles exerting its antiviral effect on several enveloped viruses during the entry step of virus infection [28]. Viruses have multiple mechanisms to inhibit or delay the expression or functions of antiviral proteins. Here we show that eight of nine studied filovirus VP24s inhibit IFN-induced activation of MxA and IFITM3 promoters. Importantly, all VP24 proteins that inhibited the MxA promoter activation also inhibited or reduced IFN-α induced expression of endogenous MxA protein.

Previous studies on EBOV VP24 have shown it to exert a strong inhibitory effect on IFN-induced pathway by binding to importin and preventing the nuclear localization of activated signalling molecule STAT1 [12, 22]. Recently, it was shown that BDBV, RESTV and LLOV VP24s have a similar mechanism of action as EBOV VP24 [13, 14]. Interestingly, it was estimated that BDBV VP24 shows a weaker binding activity to importin-α, has a reduced half-life, and exerts a decreased suppression of IFN-induced gene expression compared to EBOV and RESTV VP24s, possibly leading to differences in the pathogenicity of these filoviruses [14]. Here, we also demonstrate a strong inhibition of IFN-induced pathway by EBOV and RESTV VP24s, especially on the activation of MxA promoter. Furthermore, BDBV VP24 seems to be the weakest inhibitor of the activation of IFITM3 promoter. In addition to EBOV, BDBV, RESTV and LLOV VP24s, we show here that also BOMV, SUDV, TAFV and MLAV VP24s inhibit IFN-induced activation of MxA and IFITM3 promoters and the expression of endogenous MxA protein. Our results on NLS-mutated EBOV, BOMV, RESTV and SUDV VP24s not being able to inhibit the activation of MxA and IFITM3 promoters and the expression of endogenous MxA protein, further extends the analysis of filovirus NLS and verify the importance of importin-α binding function on the inhibitory effect of filovirus VP24s.

MARV inhibits the IFN-induced pathway with another, VP24 unrelated mechanism. MARV VP40 inhibits the phosphorylation of STATs whereas MARV VP24 apparently plays no role in the inhibition of IFN-induced pathway [15]. Similarly, we show here that MARV VP24 has no or extremely weak inhibitory effect on IFN-induced activation of MxA and IFITM3 promoters or on the expression of endogenous MxA protein, regardless of similar sub-cellular MARV VP24 location (nucleus and cytoplasm) as with other filovirus VP24s. A recent study showed a similar function for MLAV, indicating that MLAV VP40, rather than VP24, blocks IFN-induced antiviral gene expression. However, they observed a modest inhibition in IFN-induced activation with high amounts of MLAV VP24 [16]. In contrast, in the present study we observe an inhibition of activation of MxA and IFITM3 promoters and the expression of MxA by MLAV VP24. This difference could be due to expression levels of MLAV VP24, since in the previous study [16] an inhibition of ISG54 promoter was observed with high amounts of MLAV VP24. Whether these differences in inhibitory effect have any indication on pathogenicity of the filovirus species remains to be solved. We and others have utilized overexpression of one protein while in the virus infection cycle, the mechanism and inhibitory effect of a viral protein can be dependent on the presence of other proteins and on the timing of the expression of the protein.

VP24 has an important role in filovirus life cycle and in the pathogenicity of the virus. During the large West African EBOV epidemic in 2014–2015, the circulating virus isolates were sequenced and adaptive mutations linked to EBOV virulence were assessed. There were no accumulating amino acid changes in EBOV proteins interfering with interferon response [29]. Similarly, our sequence analysis here demonstrates that VP24 amino acid sequences have remained relatively unchanged. This stability implies that the functions of VP24 are essential and VP24 is likely not under an immunological pressure. The evolutionary stability of filovirus VP24 genes is essential information for antiviral drug development and thus filovirus VP24 is a potent target for antivirals, possibly even for a more broad-spectrum antivirals against several filovirus species. For example certain flavonoids have been shown to interfere with the binding of VP24 to importin-α thus restoring the IFN-induced signalling pathways of innate immune responses [30].

In summary, our study shows that all analysed filovirus VP24 proteins, except that of MARV VP24, can efficiently inhibit IFN-induced MxA and IFIMT3 promoter activation and MxA protein expression, and this inhibition is dependent of a functional cluster three in the NLS of VP24s. Our findings validate the antagonistic effects of filovirus VP24 proteins on IFN-induced pathway, providing further groundwork for future filovirus pathogenesis research and for the development of new antiviral drugs.

Funding information
This research was funded by the Academy of Finland (grant numbers 297329 and 339512), the Sigrid Jusélius Foundation and the Jane and Aatos Erkko Foundation (grant number 3067-84b53).

Acknowledgements
Soili Jussila and Sari Maljanen are acknowledged for their technical assistance.

Author contributions
Conceptualization, H.K., I.J., L.K. and M.H.; methodology, L.T., R.L., E.A., J.H. and M.H.; validation, H.K., L.T., R.L., E.A., J.H., I.J., L.K. and M.H.; formal analysis, H.K., L.T., P.K., R.L., E.A., J.H. and M.H.; investigation, H.K., L.T., P.K., R.L., E.A., J.H. and M.H.; writing—original draft preparation, H.K., L.T., P.K., R.L., L.K. and M.H; writing—review and editing, H.K., L.T., E.A., J.H., I.J., L.K. and M.H.; visualization, H.K., P.K. and M.H.; supervision, I.J., L.K. and M.H.; project administration, I.J., L.K. and M.H.; funding acquisition, I.J. and L.K. All authors have read and agreed to the published version of the manuscript.

Conflicts of interest
The authors declare no conflicts of interest. The funders had no role in the design of the study; in the collection, analyses, or interpretation of data; in the writing of the manuscript, or in the decision to publish the results.

Ethical statement
Ethical approval for animal immunization was provided by the Ethics committee of animal experimentation in Southern Finland (permission no: ESLH-ESAVI/11411/04.10.07/2014 to DVM Anna Meller).

References

1. Feldmann H, Jones S, Klenk H-D, Schnittler H-J. Ebola virus: from discovery to vaccine. *Nat Rev Immunol* 2003;3:677–685.
2. Carroll SA, Towner JS, Sealy TK, McMullan LK, Khristova ML, *et al*. Molecular evolution of viruses of the family Filoviridae based on 97 whole-genome sequences. *J Virol* 2013;87:2608–2616.
3. Amarasinghe GK, Aréchiga Ceballos NG, Banyard AC, Basler CF, Bavari S, *et al*. Taxonomy of the order Mononegavirales: update 2018. *Arch Virol* 2018;163:2283–2294.
4. Bukreyev AA, Chandran K, Dolnik O, Dye JM, Ebihara H, *et al*. Discussions and decisions of the 2012–2014 International Committee on Taxonomy of Viruses (ICTV) filoviridae study group, January 2012–June 2013. *Arch Virol* 2014;159:821–830.
5. Kuhn JH, Becker S, Ebihara H, Geisbert TW, Johnson KM, *et al*. Proposal for a revised taxonomy of the family Filoviridae: classification, names of taxa and viruses, and virus abbreviations. *Arch Virol* 2010;155:2083–2103.
6. Lam WK, Zhong NS, Tan WC. Overview on SARS in Asia and the world. *Respirology* 2003;8 Suppl:S2–5.
7. McNab F, Mayer-Barber K, Sher A, Wack A, O'Garra A. Type I interferons in infectious disease. *Nat Rev Immunol* 2015;15:87–103.
8. Au-Yeung N, Mandhana R, Horvath CM. Transcriptional regulation by STAT1 and STAT2 in the interferon JAK-STAT pathway. *JAKSTAT* 2013;2:e23931.
9. Mühlberger E. Filovirus replication and transcription. *Future Virol* 2007;2:205–215.
10. Basler CF. Innate immune evasion by filoviruses. *Virology* 2015;479–480:122–130.
11. Messaoudi I, Amarasinghe GK, Basler CF. Filovirus pathogenesis and immune evasion: insights from Ebola virus and Marburg virus. *Nat Rev Microbiol* 2015;13:663–676.
12. Xu W, Edwards MR, Borek DM, Feagins AR, Mittal A, *et al*. Ebola virus VP24 targets a unique NLS binding site on karyopherin alpha 5 to selectively compete with nuclear import of phosphorylated STAT1. *Cell Host Microbe* 2014;16:187–200.
13. Feagins AR, Basler CF. Lloviu virus VP24 and VP35 proteins function as innate immune antagonists in human and bat cells. *Virology* 2015;485:145–152.
14. Schwarz TM, Edwards MR, Diederichs A, Alinger JB, Leung DW, *et al*. VP24-Karyopherin alpha binding affinities differ between Ebolavirus species, influencing interferon inhibition and VP24 stability. *J Virol* 2017;91:e01715-16.
15. Valmas C, Grosch MN, Schümann M, Olejnik J, Martinez O, *et al*. Marburg virus evades interferon responses by a mechanism distinct from ebola virus. *PLoS Pathog* 2010;6:e1000721.
16. Williams CG, Gibbons JS, Keiffer TR, Luthra P, Edwards MR, *et al*. Impact of Měnglà virus proteins on Human and Bat innate immune pathways. *J Virol* 2020;94:e00191-20.
17. Thompson JD, Higgins DG, Gibson TJ. CLUSTAL W: improving the sensitivity of progressive multiple sequence alignment through sequence weighting, position-specific gap penalties and weight matrix choice. *Nucleic Acids Res* 1994;22:4673–4680.
18. Tamura K, Stecher G, Kumar S. MEGA11: Molecular Evolutionary Genetics Analysis version 11. *Mol Biol Evol* 2021;38:3022–3027.
19. He F, Melén K, Maljanen S, Lundberg R, Jiang M, *et al*. Ebolavirus protein VP24 interferes with innate immune responses by inhibiting interferon-λ1 gene expression. *Virology* 2017;509:23–34.
20. Ronni T, Melén K, Malygin A, Julkunen I. Control of IFN-inducible MxA gene expression in human cells. *J Immunol* 1993;150:1715–1726.
21. He FB, Khan H, Huttunen M, Kolehmainen P, Melén K, *et al*. Filovirus VP24 proteins differentially regulate RIG-I and MDA5-dependent type I and III interferon promoter activation. *Front Immunol* 2021;12:694105.
22. Reid SP, Leung LW, Hartman AL, Martinez O, Shaw ML, *et al*. Ebola virus VP24 binds karyopherin alpha1 and blocks STAT1 nuclear accumulation. *J Virol* 2006;80:5156–5167.
23. Negredo A, Palacios G, Vázquez-Morón S, González F, Dopazo H, *et al*. Discovery of an ebolavirus-like filovirus in europe. *PLoS Pathog* 2011;7:e1002304.
24. Goldstein T, Anthony SJ, Gbakima A, Bird BH, Bangura J, *et al*. The discovery of Bombali virus adds further support for bats as hosts of ebolaviruses. *Nat Microbiol* 2018;3:1486.
25. Yang X-L, Tan CW, Anderson DE, Jiang R-D, Li B, *et al*. Characterization of a filovirus (Měnglà virus) from Rousettus bats in China. *Nat Microbiol* 2019;4:543.
26. Pappalardo M, Reddin IG, Cantoni D, Rossman JS, Michaelis M, *et al*. Changes associated with Ebola virus adaptation to novel species. *Bioinformatics* 2017;33:1911–1915.
27. Haller O, Kochs G. Human MxA protein: an interferon-induced dynamin-like GTPase with broad antiviral activity. *J Interferon Cytokine Res* 2011;31:79–87.
28. Spence JS, He R, Hoffmann H-H, Das T, Thinon E, *et al*. IFITM3 directly engages and shuttles incoming virus particles to lysosomes. *Nat Chem Biol* 2019;15:259–268.
29. Dunham EC, Banadyga L, Groseth A, Chiramel AI, Best SM, *et al*. Assessing the contribution of interferon antagonism to the virulence of West African Ebola viruses. *Nat Commun* 2015;6:8000.
30. Fanunza E, Iampietro M, Distinto S, Corona A, Quartu M, *et al*. Quercetin blocks Ebola virus infection by counteracting the VP24 interferon-inhibitory function. *Antimicrob Agents Chemother* 2020;64:e00530-20.